Effects of Pacific Intertropical Convergence Zone precipitation bias on ENSO phase transition

2014 Environ. Res. Lett. 9 064008

(http://iopscience.iop.org/1748-9326/9/6/064008)

OPEN ACCESS
IOP Publishing
Environmental Research Letters
Environ. Res. Lett. 9 (2014) 064008 (8pp)
doi:10.1088/1748-9326/9/6/064008

Effects of Pacific Intertropical Convergence Zone precipitation bias on ENSO phase transition

Yoo-Geun Ham[1] **and Jong-Seong Kug**[2]

[1] Faculty of Earth Systems and Environmental Sciences, Chonnam National University, Gwang-ju, Korea
[2] School of Environmental Science and Engineering, Pohang University of Science and Technology (POSTECH), Pohang, Korea

E-mail: jskug1@gmail.com

Received 20 November 2013, revised 2 May 2014
Accepted for publication 14 May 2014
Published 9 June 2014

Abstract

In this study, the effect of mean precipitation bias over the Pacific Intertropical Convergence Zone (ITCZ) on the El Niño southern oscillation (ENSO) transition is examined using CMIP3 and CMIP5 archives. It is found that the climate models with excessive mean precipitation over the central/eastern Pacific ITCZ tend to simulate slower phase transition of the ENSO. This is because a wetter climatology provides a favorable condition for anomalously strong convective activity; the El Niño-related convection anomaly tends to be increased over the central/eastern Pacific ITCZ with a local wet bias. This induces additional low-level westerlies over the central/eastern equatorial Pacific. As a result, the ENSO-related zonal wind stress anomaly over the central Pacific, which is south of the equator without the wet ITCZ bias during boreal winter, is shifted to the east, and its meridional width is expanded northward. It is found that both the eastward shift and northward expansion of ENSO-related wind stress can lead to slower ENSO phase transition as it takes longer time for the reflected Rossby waves to suppress the ENSO growth. This implies that the off-equatorial mean precipitation plays an important role in ENSO phase transition.

Keywords: ITCZ, ENSO, climate models, CMIP5

1. Introduction

Even though there have been progress, it is still a challenge to simulate realistic mean tropical climate in coupled general circulation models (CGCMs) (AchutaRao and Sperber 2002, 2006). Especially, most CGCMs still have difficulty in reproducing the observed intensity of the mean tropical precipitation over the Intertropical Convergence Zone (ITCZ), the South Pacific Convergence Zone (SPCZ), and over the warm pool area (Lin 2007, Bellucci *et al* 2010).

Many studies argued that the mean atmospheric state over the tropics can determine the simulated ENSO characteristics (Schneider 2002, Guilyardi 2006, Guilyardi *et al* 2004, 2009, Kim *et al* 2008, 2011, Lloyd *et al* 2009, Kug and Ham 2011, Watanabe *et al* 2011, Jang *et al* 2013). Guilyardi (2006) analyzed CMIP3 models and showed that the models with strong El Niño amplitude tend to have a weak mean trade wind, supporting the views of Fedorov and Philander (2001) and Burgers and van Oldenborgh (2003). This weak mean trade wind is directly linked to the smaller zonal temperature gradient with reduced (increased) precipitation over the western (eastern) Pacific (Fedorov and Philander 2001).

In addition, Watanabe *et al* (2011) emphasized the role of mean precipitation over the eastern equatorial Pacific on ENSO amplitude and frequency using a series of experiments with different convective parameters in the CGCM of Model for Interdisciplinary Research on Climate (MIROC). They showed that the ENSO-related wind anomalies are shifted to

the west due to the excessive dry bias over the eastern equatorial Pacific, thereby making the Bjerknes feedback less effective. They argued that this dryness over the eastern equatorial Pacific is controlled by the strength of the ITCZ, as the strength of the ITCZ determines that of the subsidence over the equatorial cold tongue region. It implies that the mean ITCZ precipitation can affect ENSO characteristics in CGCMs. Since most of the CGCMs have stronger precipitation biases off the equator than over the equator (Lin 2007), it is also worthwhile to examine the effect of the ITCZ bias on simulated ENSO.

With these motivations, this paper will analyze CMIP3 and CMIP5 outputs to illustrate how the strength of the ITCZ changes the ENSO characteristics by modulating ENSO-related atmospheric and oceanic responses. In section 2, descriptions of the observational data and the CGCM used in this study are provided. The impacts of ITCZ strength on ENSO-related anomalies, and on ENSO period will be shown in sections 3 and 4, respectively. A summary and discussions are presented in section 4.

2. Data and model

We analyzed a total of 42 climate models, which consist of 21 models from historical runs of CMIP5, and 21 models from the 20c3m simulations of CMIP3, the same as in Kug *et al* (2012). Only one ensemble member per model is used in this study. For comparison with the model results, we used observed precipitation data of the Global Precipitation Climatology Project (GPCP) from 1980 to 2009 (Adler *et al* 2003).

3. Effect of Pacific ITCZ strength on ENSO-related anomalies

Before assessing the effects of Pacific ITCZ strength on the ENSO, we first examined the climatological precipitation in the CMIP archives. Figure 1(a) shows the precipitation bias in multi-model ensemble (MME) during December–February (DJF). As Lin (2007) pointed out, there are positive biases of climatological precipitation over the off-equatorial regions and the Maritime Continent. The positive bias over the northern off-equator region (denoted by a red box) approaches 3 mm day^{-1}, indicating that the climate models tend to have stronger ITCZ over central/eastern Pacific than the observed. Also, the wet bias over the southern off-equator region is zonally elongated from the western to the eastern Pacific, which implies that the simulated SPCZ often looks like the ITCZ in the CGCMs, so called 'double ITCZ' problem (Lin 2007). On the other hand, there is a dry bias over the western equatorial Pacific between 150–180 °E.

In addition to the MME bias, we calculated an inter-model spread using the standard deviation (STD) of DJF-mean precipitation differences of each model from the MME value (figure 1(b)). In general, the locations with relatively large MME biases are well matched to those with large inter-model differences. For example, over the off-equatorial central Pacific between 14–10 °S and western equatorial Pacific, the STD of mean precipitation approaches 3 mm day^{-1}. In addition, over the ITCZ region, the STD of mean precipitation difference from the MME is about 3 mm day^{-1}, which is as large as the MME bias. This shows that the ITCZ over the central/eastern Pacific is one of the regions where the biases and inter-model differences are the biggest.

To investigate the effect of the ITCZ bias in more detail, we first define the ITCZ index as the differences of the DJF-mean precipitation between off-equatorial (i.e., the red box of 170 – 110 °W, 4–10 °N) and central/eastern equatorial Pacific (i.e., the blue box of 170 – 110 °W, 3 °S–3 °N). Then, among the 42 climate models, we selected 10 models that have the smallest and biggest ITCZ indices, respectively, to examine the difference in the ENSO characteristics with respect to the ITCZ index. For simplicity, the group with the smallest ITCZ indices will be denoted as 'moderate ITCZ models' as the strength of the ITCZ in these models is similar to the observed, and that with the biggest ITCZ indices will be denoted as 'strong ITCZ models'.

Figures 1(c)–(e) show the DJF-mean precipitation in the GPCP, 'moderate ITCZ models' and 'strong ITCZ models'. The observed precipitation pattern shows a strong precipitation over the ITCZ, the SPCZ, and the maritime continent (figure 1(c)). The 'moderate ITCZ models' can capture the major observed features well, but they tend to have a wet bias in general, and the double ITCZ problem. However, the magnitude of the precipitation over the ITCZ in these models is quite similar to the observed. On the other hand, the 'strong ITCZ models' can simulate excessive precipitation over the ITCZ region. It is noted that the ITCZ precipitation is even larger than that over the SPCZ region, unlike the observed and the 'moderate ITCZ models'. In addition, it is also clear that the 'strong ITCZ models' tend to underestimate the equatorial precipitation over the central Pacific, so that the equatorial dry zone is excessively expanded to the western Pacific, which is closely related to ENSO variability (Watanabe *et al* 2011, Jang *et al* 2013). In general, the 'moderate ITCZ models' tend to have a better agreement with the observed precipitation than the 'strong ITCZ models'.

Our goal is to examine how these biases in climate models affect ENSO variability. To do this, we firstly checked the atmospheric responses associated with the ENSO because the mean precipitation can directly affect the anomalous atmospheric response to ENSO SST forcing (Kim *et al* 2011). Figure 2 shows the linear regressions of anomalous SST, precipitation, zonal wind stress onto the Niño3 index (150–90 °W, 5 °S–5 °N) during DJF in 'moderate' and 'strong ITCZ models'. Note that these regressions denote the changes in SST, precipitation, and zonal wind stress due to unit change of the Niño3 index. This means that the SST amplitude is normalized to one degree over the Niño3 area, so that the ENSO amplitude cannot be compared in this regression. In the 'moderate ITCZ models', the ENSO-related SST anomalies are clearly shown over the

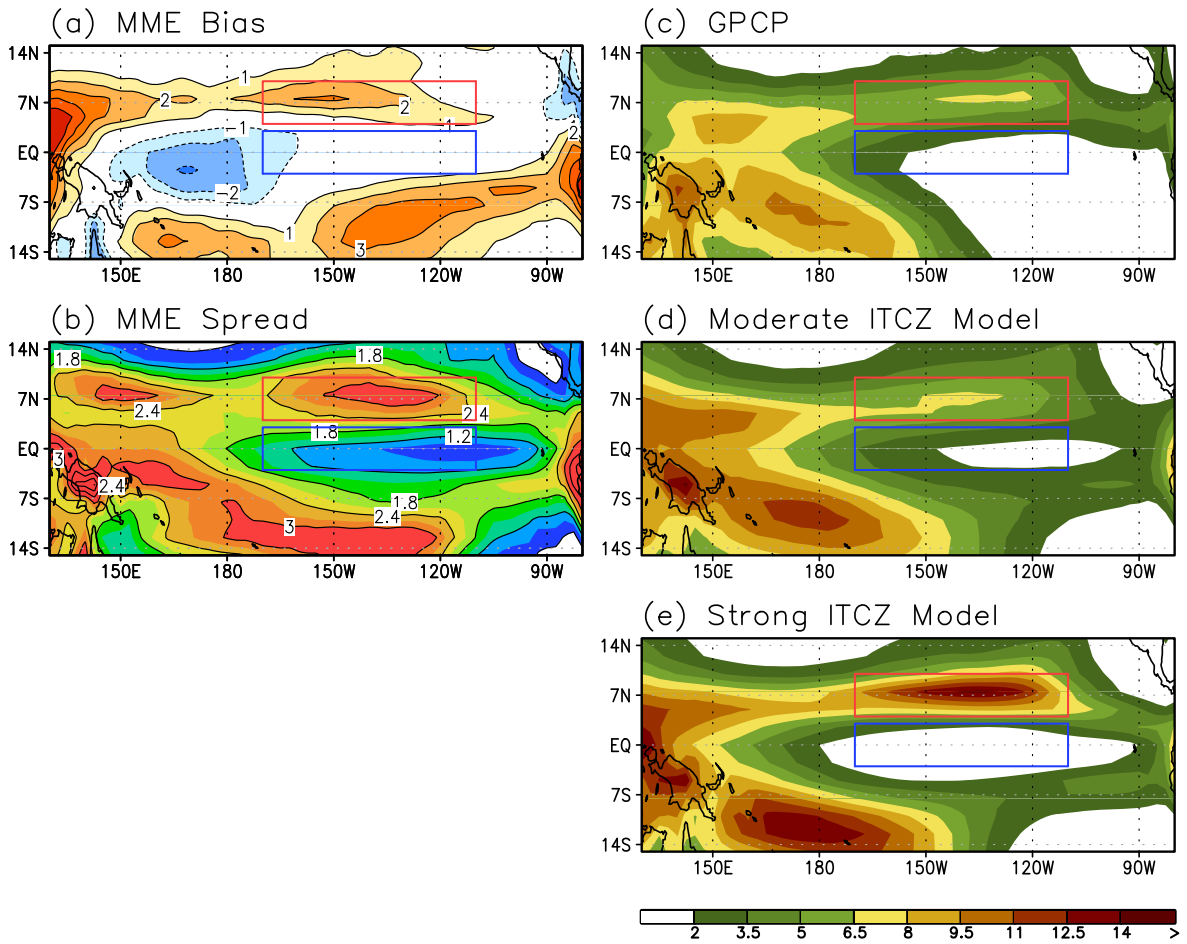

Figure 1. (a) Multi-model ensemble (MME) bias of DJF precipitation. (b) Standard deviation (STD) of DJF precipitation differences of each model from the MME. The climatological precipitation during DJF in (c) GPCP, (d) 'moderate ITCZ model' group, and (e) 'strong ITCZ model' group.

central/eastern Pacific between 170 °E–120 °W. Due to this SST forcing, there is a positive precipitation anomaly around 180 °E, and the latitudinal center is slightly shifted to the south of the equator (Harrison and Vecchi 1999, Vecchi and Harrison 2003).

The pattern of SST anomalies in the 'strong ITCZ models' is similar to that in the 'moderate ITCZ models', though it is slightly extended to the western Pacific. Most striking differences are found in the precipitation patterns of these two groups. First, the precipitation anomalies along the equator in the 'strong ITCZ models' are shifted to the west compared to those in the 'moderate ITCZ models'. This is possibly related to the expansion of the equatorial dry zone as shown in figure 1(e), which makes the anomalous convection confined in the western Pacific. Once the mean convective activity is confined over the western Pacific, positive El Niño SST anomalies over the eastern Pacific cannot increase local convection effectively; therefore, the convective anomaly to the El Niño SST forcing is shifted to the west (Watanabe *et al* 2011, Ham and Kug 2012, Kug *et al* 2012). In summary, the equatorially averaged (5 °S–5 °N) ENSO-related precipitation anomaly in the 'strong ITCZ models' is shifted to the west compared to that in the 'moderate ITCZ models' (figure 2(c)).

Secondly, in the 'strong ITCZ models' there is a strong and peculiar precipitation anomaly over the central/eastern Pacific ITCZ region near 5 °N, 150–120 °W. It seems obvious that this is related to the strong wet bias over the ITCZ in the 'strong ITCZ models', because the wet bias over the ITCZ provides a more favorable condition to increase the local precipitation anomaly in response to the SST change. This strong off-equatorial precipitation anomaly induces a unique wind response, which directly affects the ENSO characteristics.

As shown in figures 2(d) and (e), the anomalous westerly prevails over the central equatorial Pacific as a response to the enhanced convective activity over the central Pacific at the south of the equator in both groups. The distinctive difference in zonal wind stress response between the two groups is that the eastern part of the westerly wind anomalies is elongated to the northeast over the central/eastern Pacific in the 'strong ITCZ models'. For example, the westerly wind stress anomaly between 150–120 °W is stronger north of the equator in the 'strong ITCZ models', while that is quite weak at the north of the equator in the 'moderate ITCZ models'. These

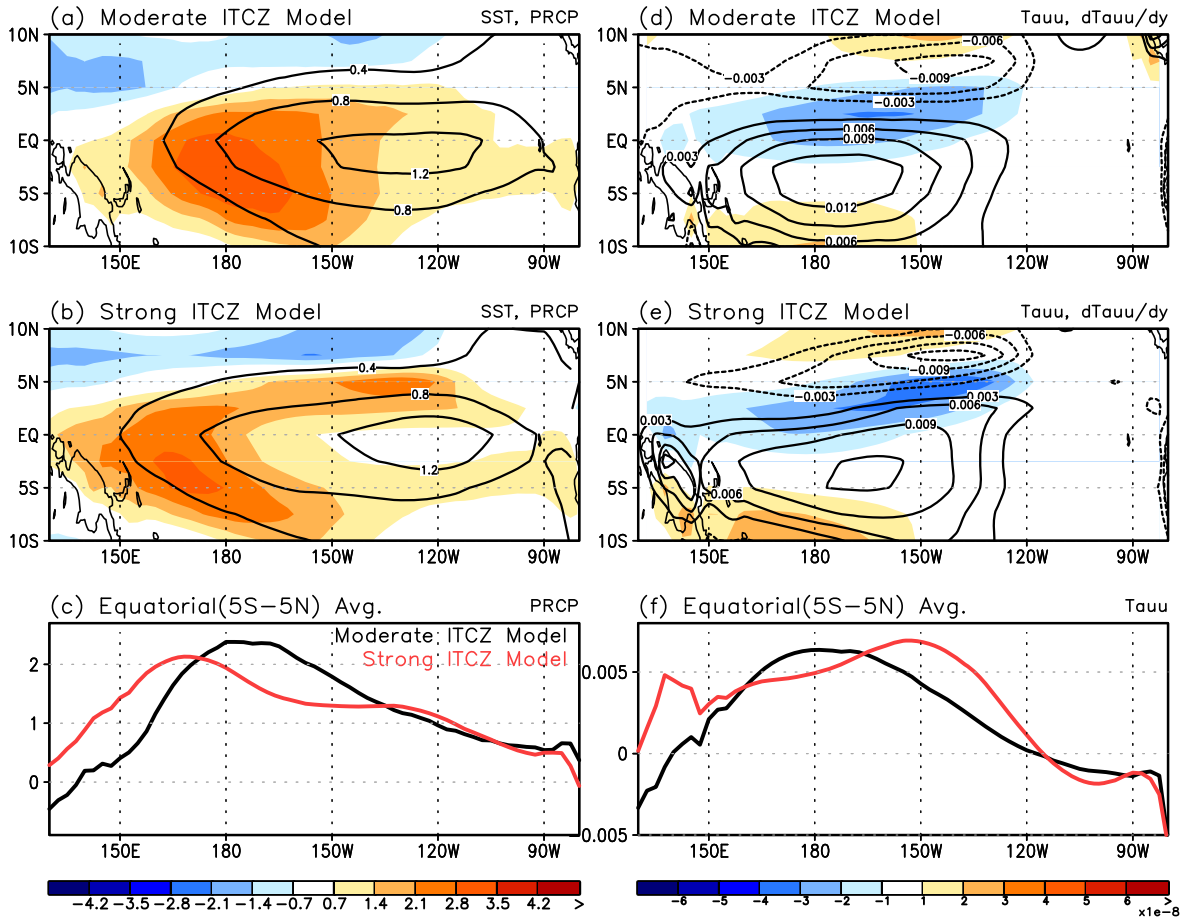

Figure 2. Regression of SST (°C/°C; contour) and precipitation (mm day^{-1} per °C; shading) anomaly onto Niño3 index during DJF in (a) 'moderate ITCZ model' and (b) 'strong ITCZ model' groups. The regression of zonal mean wind stress anomaly (N m^{-2} per °C; contour) and meridional gradient of zonal wind stress anomaly (N m^{-2} per °C m^{-1}; shading) onto Niño3 index during DJF in (d) 'moderate ITCZ model' and (e) 'strong ITCZ model' groups. The equatorial average (5 °S–5 °N) of regressed precipitation and zonal wind stress anomaly in the two model groups are shown in (c) and (f), respectively.

features are closely related to the enhanced anomalous convection over the ITCZ region, which induces low-level westerly as a Gill-type response (Gill 1980). This means that the off-equatorial precipitation anomaly in the 'strong ITCZ models' causes systematic differences in the wind responses during the ENSO.

This additional westerly wind stress anomaly over the central/eastern Pacific ITCZ in the 'strong ITCZ models' can play a critical role in modulating ENSO characteristics. That is, in the 'strong ITCZ models,' the equatorially averaged (5 °S–5 °N) zonal wind stress is shifted to the east although the equatorial precipitation is located to the west, compared with that in the 'moderate ITCZ models' (figures 2(c), (f)). Note that this result is not changed much for the narrower equatorial band (i.e. 3 °S–3 °N). Once the wind stress anomalies are shifted to the east, westerly wind stress forcing shoals off-equatorial thermocline eastward and effectively deepens the equatorial thermocline over the eastern Pacific suggesting a stronger and longer El Niño (An and Wang 2000, Kang and Kug 2002). In addition, the zonally-averaged zonal wind is greater in the strong ITCZ model, which also lead to deepened thermocline over the eastern Pacific.

In addition to the eastward shift, this additional equatorial westerly anomaly in the 'strong ITCZ models' shifts the wind stress curl to the north. That is, the maximum negative wind stress curl (shading in figures 2(d), (e)) between 150 °W and 120 °W is around 2 °N in the 'moderate ITCZ models,' while that is located at 5 °N in the 'strong ITCZ models.' Because the wind stress curl can deepen the off-equatorial thermocline depth through upwelling Rossby waves (Wang and An 2001), the additional westerly and associated wind stress curl may alter the structure of off-equatorial thermocline, which affects the phase transition of the ENSO, because the off-equatorial thermocline anomalies can lead to the subsequent ENSO event (Battisti and Hirst 1989, Jin 1997).

To examine this hypothesis in more detail, figure 3 shows the lag-regression of 20 °C isotherm depth (i.e., Z20) during SON, DJF, and the subsequent MAM onto the DJF Niño3 index. In the 'moderate ITCZ models,' there is an east-west see-saw pattern of Z20 during SON over the equatorial Pacific. In addition, the negative Z20 anomaly is along the ITCZ between 5–10 °N. During DJF, this off-equatorial

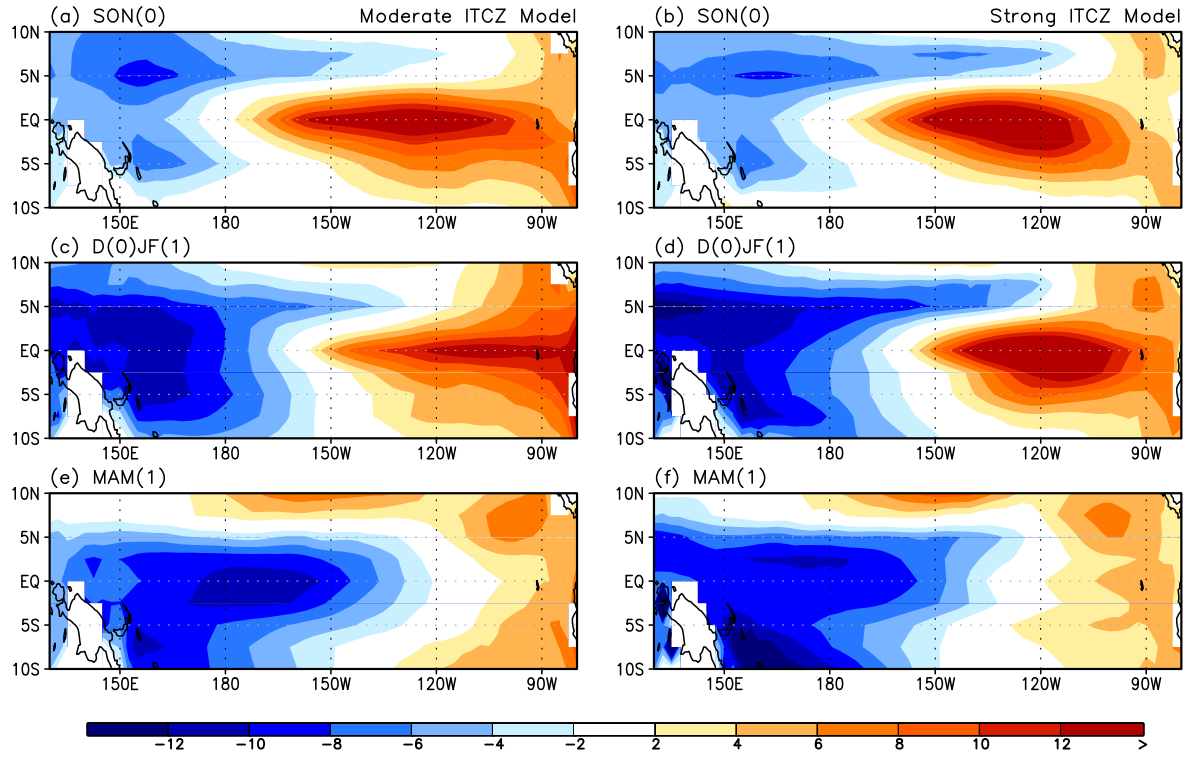

Figure 3. Regressions of 20 °C isotherm depth (m °C^{-1}) during (a) SON(0), (c) D(0)JF(1), and (e) MAM(1) onto D(0)JF(1) Niño3 anomaly in the 'moderate ITCZ model' group. Regressions of 20 °C isotherm depth in the 'strong ITCZ model' group for (b) SON(0), (d) D(0)JF(1), and (f) MAM(1) are also shown.

thermocline shoaling is slightly retreated to the west, and the negative anomalies over the western Pacific are centered at the equator, possibly due to the western boundary reflection of the upwelling Rossby wave (Battisti and Hirst 1989), or due to the discharge of equatorial heat content (Jin 1997). During the subsequent MAM, the center of negative Z20 is at the equator, implying that the ENSO transition process works successfully in the 'moderate ITCZ models,' and this negative Z20 signal over the equator propagates eastward, leading to the La Niña signal during the subsequent seasons (Jin 1997).

The 'strong ITCZ models' show similar evolutions of anomalous thermocline, but distinctive differences are evident north of the equator. During SON, the negative Z20 over the northern off-equator region is slightly stronger than that in the 'moderate ITCZ models'. This difference is clearer during DJF; the negative Z20 signal remains along the ITCZ region in the 'strong ITCZ models'. In addition, the negative thermocline in the 'strong ITCZ models' is located at slightly higher latitude than that in the 'moderate ITCZ models', consistent with the location of the anomalous wind stress curl in figures 2(d) and (e). Due to the decreasing Rossby wave phase speed with increasing latitude, the upwelling Rossby wave, associated with the negative Z20 over the northern off-equatorial region, will propagate more slowly in the 'strong ITCZ models', leading to a longer adjustment process.

Because of the slower Rossby wave phase speed at higher latitudes, and the eastward-shifted Rossby wave excitation point, it takes a longer time for the negative Z20 signal to reach the western boundary; so the ENSO phase transition becomes slower in the 'strong ITCZ models'. The maximum negative thermocline in the 'strong ITCZ models' is still located off-equator during MAM, while that of the 'moderate ITCZ models' is at equator. As the negative thermocline depth anomaly in 'moderate ITCZ models' is propagated from the off-equator to equator, the subsequent La Niña signal is initiated from MAM season. On the other hand, as the off-equatorial negative thermocline is still robust, the subsequent La Niña signal is not initiated yet until MAM season in 'strong ITCZ model'. Therefore, the transition to the La Niña in 'strong ITCZ model' is slower than that in 'moderate ITCZ model'. This implies that the discharge of equatorial heat content during the ENSO is systematically slower in the 'strong ITCZ models' due to the enhanced westerly wind forcing over the central/eastern Pacific.

4. Impact of ITCZ strength on ENSO

In section 3, we argued that there are substantial impacts of the climatological ITCZ precipitation on ENSO-related anomalies, that is, (1) the eastward shift of the zonal wind stress and (2) northward expansion of zonal wind stress. These changes consistently act to slow down the ENSO phase transition (Kirtman 1997, Capotondi *et al* 2006). To confirm these changes lead to distinct ENSO evolution between the two model groups, figure 4 shows the time evolution of Niño3 index in the 'moderate' and the 'strong ITCZ models' using the lag composite with respect to the DJF Niño3 SST. Note

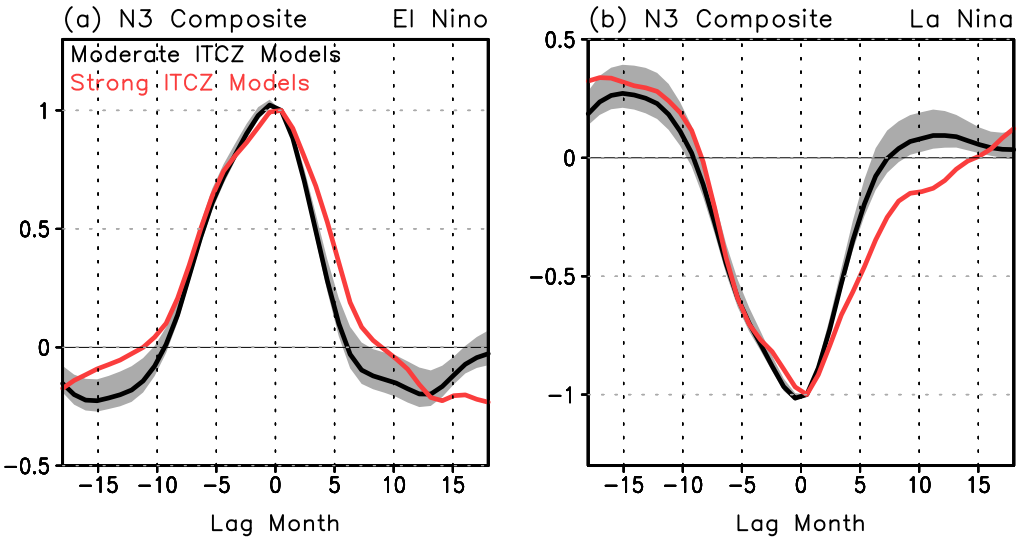

Figure 4. (a) The time evolution of Niño3 index during the El Niño events in 'moderate ITCZ model' (black line) and 'strong ITCZ model' (red line) groups using the lagged composite with respect to the DJF Niño3. (b) Same as (a), but for La Niña events.

that the definition of the El Niño (La Niña) is when the DJF Niño3 is larger (smaller) than one (minus one) STD, and the Niño3 index at lag 0 is normalized to focus on the ENSO period. Each composite is obtained from the 10 models average.

During both El Niño and La Niña events, it is clear that the ENSO transition in the 'strong ITCZ models' is significantly slower than that in the 'moderate ITCZ models'. For example, in the El Niño composite, the normalized Niño3 index changes the sign from positive to negative at +9 month lag in the 'strong ITCZ models', on the other hand, that is at +6 month lag in the 'moderate ITCZ models'. Similarly, during the La Niña event, the Niño3 index changes the sign at +7 month lag in the 'moderate ITCZ models', while it changes sign at +15 month lag in the 'strong ITCZ models'. This difference is significant with 95% confidence level using the *t*-test based on the STD of 42 models' differences from the MME value. We also checed that the the power spectrum result shows that the 'strong ITCZ models' tend to have longer period of ENSO, compared to that of the 'moderate ITCZ models' (not shown).

Note that the ENSO magnitude is stronger in the 'strong ITCZ models'. The composite Niño3 index during the El Niño peak phase (i.e., DJF) is 1.45 °C and 1.10 °C in 'strong' and 'moderate ITCZ models', respectively. Also, the composited Niño3 index during the La Niña peak season is stronger in the 'strong ITCZ models' (i.e., −1.22 °C), compared to that in the 'moderate ITCZ models' (i.e., −1.01 °C). This is consistent with the result in Kang and Kug (2002) that the eastward shift of ENSO-related zonal wind stress anomaly leads to a stronger ENSO with a longer period.

5. Summary and discussions

In this study, the role of mean precipitation over the Pacific ITCZ in determining ENSO period is examined using CMIP3 and CMIP5 archives. The 'strong ITCZ models' tend to simulate excessive ENSO-related convective responses over the central/eastern Pacific ITCZ. This enhanced anomalous convection leads to additional low-level westerlies over the central/eastern equatorial Pacific as a Gill-type response. This leads to eastward shift of atmospheric wind forcing, which is associated with a slow phase transition of ENSO by delaying its decaying mechanism. Also, the northward expansion of zonal wind stress anomaly in the 'strong ITCZ models' indicates a widening of zonal wind stress in the meridional direction during the boreal winter of ENSO events. This widening makes the equatorial discharge process of heat content slower due to the decreasing phase speed of off-equatorial Rossby waves with increasing latitude; then, it acts to retard the ENSO transition. It means that the eastward shift and northward expansion of ENSO-related westerly forcing due to excessive ITCZ mean precipitation consistently act to lead a slower ENSO transition, which might lead to a longer ENSO.

Recently, Watanabe *et al* (2011) discussed the effect of ITCZ strength on ENSO characteristic based on the their single model experiments with different physical parameter. They showed that a strong ITCZ leads to a strong sinking motion over the equatorial cold tongue region by developing local Hadley cell, so that the anomalous convective response over the cold tongue region becomes insensitive which shift the ENSO-related convection to the west. In the MME of this study, this process seems to work. For example, the precipitation pattern is shifted to the west for the strong ITCZ models. However, strong ITCZ models show the equatorial wind anomalies are further expanded to the east, which is inconsistent with the argument in Watanabe *et al* (2011). This inconsistency is possibly related to the pattern of the excessive ITCZ. In Watanabe *et al* (2011)'s experiments, the precipitation changes are strong near 10 N. However, the multi-model in our study showed strong wet bias near 7 °N. If the location is far from the equator, it will be hard to produce off-

equatorial precipitation anomalies in the response to equatorial SST anomalies. This can make the difference in the effect of the strong ITCZ. In addition, the magnitude of ITCZ change may also explain the difference. In Watanabe *et al* (2011), as shown in their figures 7(e) or (h), the change in mean precipitation among experiments is about 1 mm day^{-1} both over the ITCZ and equatorial cold tongue area (shown in contour). And, the ratio of precipitation change to mean precipitation (denoted as shading) is less than 10% over the ITCZ area, while that is over 50% over the equatorial cold tongue. We checked the same quantity using CMIP archives (not shown here). It is found that the precipitation difference in strong ITCZ models from MME is much stronger over ITCZ in CMIP analysis, while that in cold tongue region is similar. The ratio of precipitation change to mean precipitation in analysis using CMIP archives is about 50% over the ITCZ. It implies that the 'direct ITCZ impact' would be much stronger in analysis using CMIP models than that in Watanabe *et al* (2011), so that the eastward shift of ENSO-related anomalies would be clear in this study.

In addition to the ITCZ, one wonders whether there is an impact of wet bias between 14–7 °S (figure 1(a)). To test this, we performed a similar analysis by modifying the ITCZ index to focus on the Southern Hemisphere; however, there were no significant differences in ENSO amplitude and period (not shown). Based on our study, this might be due to two factors. First, the center of zonal wind stress is already at the south of the equator during DJF, further southward shift of zonal wind stress due to excessive SPCZ precipitation may not affect the tropical wind stress forcing. Second, the discharge of equatorial heat content is effective in the northern hemisphere (Kug *et al* 2003), the changes in the discharge process over the Southern Hemisphere may have less impact on ENSO transition.

The seasonal differences in the meridional location of ENSO-related zonal wind stress are reported to be crucial in determining the ENSO peak season (Harrison and Vecchi 1999, Vecchi and Harrison 2003). Harrison and Vecchi (1999) pointed out that the ENSO-related wind stress forcing is symmetric about the equator in October–November, and then moves south of the equator in December–January, which may be important to the El Niño termination by reducing the equatorial air–sea coupling strength. It means that the southward shift of zonal wind stress is an indicator of the ENSO termination. However, the additional equatorial westerly wind stress in the 'strong ITCZ models' prevents clear southward shift of ENSO-related zonal wind stress during boreal winter season (figure 2(e)). According to Harrison and Vecchi (1999), it might cause continuous growing of ENSO SST anomalies to lead to a longer ENSO, which is also the conclusion of our study.

Acknowledgment

This research is supported by project NIMR-2012-B-2 (Development and Application of Methodology for Climate Change Prediction).

References

AchutaRao K and Sperber K 2002 Simulation of the El Niño southern oscillation: results from the coupled model intercomparison project *Clim. Dyn.* **19** 191–209

AchutaRao K and Sperber K 2006 ENSO simulation in coupled ocean-atmosphere models: are the current models better? *Clim. Dyn.* **27** 1–15

Adler R F *et al* 2003 The version 2 global precipitation climatology project (GPCP) monthly precipitation analysis (1979-present) *J. Hydrometeor.* **4** 1147–67

An S-I and Wang B 2000 Interdecadal change of the structure of the ENSO mode and it impact on the ENSO frequency *J. Clim.* **13** 2044–55

Battisti D S and Hirst A C 1989 Interannual variability in the tropical atmosphere–ocean system: influence of the basic state, ocean geometry, and nonlinearity *J. Atmos. Sci.* **46** 1687–712

Bellucci A, Gualdi S and Navarra A 2010 The double-ITCZ syndrome in coupled general circulation models: the role of large-scale vertical circulation regimes *J. Clim.* **23** 1127–45

Burgers G and van Oldenborgh G J 2003 On the impact of local feedbacks in the central Pacific on the ENSO cycle *J. Clim.* **16** 2396–407

Capotondi A, Wittenberg A and Masina S 2006 Spatial and temporal structure of tropical Pacific interannual variability in 20th century climate simulations *Ocean Model.* **15** 274–98

Federov A V and Philander S G 2001 A stability analysis of tropical ocean–atmosphere interactions: bridging measurements and theory for El Niño *J. Clim.* **14** 3086–101

Gill A E 1980 Some simple solutions for the heat induced tropical circulation *Quart. J. Meterol. Soc.* **106** 447–62

Guilyardi E 2006 El Niño—mean state—seasonal cycle interactions in a multi-model ensemble *Clim. Dyn.* **26** 229–348

Guilyardi E, Gualdi S, Slingo J M, Navarra A, Delecluse P, Cole J, Madec G, Roberts M, Latif M and Terray L 2004 Representing El Niño in coupled ocean-atmosphere GCMs: the dominant role of the atmospheric component *J. Clim.* **17** 4623–9

Guilyardi E, Braconnot P, Jin F-F, Kim S T, Kolasinski M, Li T and Musat I 2009 Atmosphere feedbacks during ENSO in a coupled GCM with a modified atmospheric convection scheme *J. Clim.* **22** 5698–718

Ham Y-G and Kug J-S 2012 How well do current climate models simulate two-types of El Niño? *Clim., Dyn.* **39** 383–98

Harrison D E and Vecchi G A 1999 On the termination of El Niño *Geophys. Res. Lett.* **26** 1593–6

Jang Y-S, Kim D, Kim Y-H, Kim D-H, Watanabe M, Jin F-F and Kug J-S 2013 Simulation of two types of El Niño from different convective parameters *Asia-Pac. J. Atmos. Sci.* **49** 193–9

Jin F F 1997 An equatorial ocean recharge paradigm for ENSO. part I: conceptual model *J. Atmos. Sci.* **54** 811–29

Kang I-S and Kug J-S 2002 El Niño and La Niña SST anomalies: asymmetric characteristics associated with their wind stress anomalies *J. Geophy. Res.* **107** 4372

Kim D, Kug J-S, Kang I-S, Jin F-F and Wittenberg A 2008 Tropical Pacific impacts of convective momentum transport in the SNU coupled GCM *Clim. Dyn.* **31** 213–26

Kim D, Jang Y-S, Kim D-H, Kim Y-H, Watanabe M, Jin F-F and Kug J-S 2011 El Niño–southern oscillation sensitivity to cumulus entrainment in a coupled general circulation model *J. Geophys. Res.* **116** D22112

Kirtman B P 1997 Oceanic Rossby wave dynamics and the ENSO period in a coupled model *J. Clim.* **10** 1690–704

Kug J-S and Ham Y-G 2011 Are there two types of La Niña events? *Geophy. Res. Lett.* **38** L16704

Kug J-S, Ham Y-G, Lee J-Y and Jin F-F 2012 Improved simulation of two types of El Niño in CMIP5 models *Environ. Res. Lett.* **7** 034002

Kug J-S, Kang I-S and An S-I 2003 Symmetric and antisymmetric mass exchanges between the equatorial and off-equatorial Pacific associated with ENSO *J. Geophys. Res.* **108** 3284

Lin J-L 2007 The double-ITCZ problem in IPCC AR4 coupled GCMs: ocean–atmosphere feedback analysis *J. Clim.* **20** 4497–525

Lloyd J, Guilaydi E, Weller H and Slingo J 2009 The role of atmosphere feedbacks during ENSO in the CMIP3 models *Atmos. Sci. Let.* **10** 170–6

Schneider E K 2002 Understanding differences between the equatorial Pacific as simulated by two coupled GCMs *J. Clim.* **15** 449–69

Vecchi G and Harrison D 2003 On the termination of the 2002–03 El Niño event *Geophys. Res. Lett.* **30** 1964

Wang B and An S-I 2001 Why the Properties of El Niño changed during the late 1970s *Geophys. Res. Lett.* **23** 3709–12

Watanabe M, Chikira M, Imada Y and Kimoto M 2011 Convective control of ENSO simulated in MIROC *J. Clim.* **24** 543–62